

## **Refractivity Data Fusion Annual Report**

Ted Rogers  
SPAWAR SC Pacific  
Atmospheric Propagation Branch  
53560 Hull Street  
San Diego, CA 92152-5001  
phone: (619) 553-1416  
email: [trogers@spawar.navy.mil](mailto:trogers@spawar.navy.mil)

Tracy Haack  
Naval Research Laboratory  
Marine Meteorology Division  
7 Grace Hopper Drive  
Monterey, CA 93943-5502  
phone: (831) 656-4727  
email: [tracy.haack@nrlmry.navy.mil](mailto:tracy.haack@nrlmry.navy.mil)

Award Number: N00014WX20585, N00014WX20044, N00014WX20579

### **LONG-TERM GOALS**

Fuse refractivity inferred from electromagnetic (EM) propagation observations with background fields from numerical weather prediction (NWP) models to create a tactical decision aid with improved battlespace awareness.

### **OBJECTIVES**

Develop data fusion method for atmospheric refractivity scheme based on objective analysis. Develop means to map observations of refractivity based on radio frequency (RF) propagation measurements into the space utilized for the analysis. Incorporate refractivity from clutter (RFC) algorithms to provide observational input to Refractivity Data Fusion (RDF) algorithm. Exercise the data fusion scheme on a combination of synthetic and real data to assess performance. Achieve reasonable processing time (on the order of 1-minute) with a representative domain size using a high-end laptop computer.

### **APPROACH**

An initial approach to estimation of atmospheric surface layer parameters by fusing radar clutter data with ensemble predictions from NWP is described in [1]. We now describe fusing EM observations with NWP background for the region above the surface layer (that includes surface based ducts and elevated ducts). This more complex, nonlinear problem involves:

1. Mapping from the space of EM signal enhancement (typically dBs) into the space of modified refractivity, which can be highly non-linear.
2. Mapping from 3-dimensional refractivity space of NWP output to the diagnostic parameter space of EM inverse method implementations (e.g., refractivity-from-clutter), such as the trapping layer height and the M-deficit (the change in refractivity across a trapping layer).
3. Performing an objective analysis in the diagnostic space which can account for possible vertical displacement, thereby preserving ducting features.

Due to the degree of non-linearity in the problem, it is doubtful that a best approach can be analytically

arrived at, as was the case for RFC. Rather, how to best implement the problem of performing an objective analysis for refractivity is amenable to a variety of alternative approaches.

In this project, a hybrid 3- and 2-dimensional variational analysis scheme (3D/2D-VAR) [2 and 3] is implemented. We start with the Cartesian representation of refractivity generated by the COAMPS model, referred to here as prognostic representation. We utilize diagnostic routines to find heights and modified refractivity values for inflection points associated with trapping layers for each vertical refractivity profile in the prognostic refractivity volume. For our purposes, the diagnostic variables are derived from the profiles of meteorological variables listed in Table 1. The diagnostic variables facilitate direct operations on the heights and gradients of trapping layers. It should be noted, though, that diagnostic variables only represent the features that are important in EM propagation. For example, if a surface based duct were present with the top of the duct at 200 meters, then only the lower 200 meters of the refractivity profile would be characterized by the diagnostic variables so it would not be unusual for the diagnostic variables to not contain features above 200-or-so meters. The result is that the 3-D prognostic representation is characterized by 2-D diagnostic representation.

The mapping from the space of the prognostic values to the space of the diagnostic values is unique; that is not necessarily so in the other direction. The process flow is as follows:

1. Profiles of COAMPS meteorological variables (modified refractivity, surface and surface-air temperature, surface winds) are used to populate the prognostic background representation.
2. Algorithms calculate the diagnostic variables associated with each NWP grid box from the prognostic representation.
3. Utilizing RFC, observations of EM propagation are mapped into space of the diagnostic variables. The diagnostic variables chosen (Table 1) are quantities typically utilized in inversions of refractivity from signal power measurements and inversion of refractivity from radar clutter.
4. An objective analysis is performed in the space of the diagnostic variables. This results as is standard for objective analysis in an adjustment to the 2-D diagnostic representation over the domain.
5. In a step referred to as vertical integration, the analysis on the diagnostic variables is mapped into the space of the prognostic variable (profiles of modified refractivity) at each grid box in the original NWP domain.

Both the prognostic background values and the diagnostic analysis values are used to generate a feature preserving (i.e., preserving the features of the original prognostic profile) analysis in the space of the prognostic variables.

## **WORK COMPLETED**

The structure of RFC has been adopted and integrated into the RDF framework, providing parameters related to the profiles of refractivity that are important to radar propagation. Also, RFC produces properties of both evaporation and surface-based ducts. RDF has been developed so that it can run end-to-end with arbitrary input on some subset of the duct diagnostic parameters. We have generated a set of ensemble predictions from COAMPS NWP, which is instrumental in understanding the spatial and temporal variability and inter-relations of the diagnostic parameters. These ensembles have allowed us to develop an understanding of the background covariance between diagnostic parameters, which is an important input for RDF. From the WALLOPS 2000 campaign, we have processed and analyzed 190 helicopter profiles of temperature and humidity, which gives us an indication of the fidelity of the RFC and RDF algorithms. Additionally, we have calculated duct properties for 119 retrievals of radar clutter

from the SPANDAR instrument located at Wallops Island, VA. Our research in RDF and RFC has been outlined in two abstracts for presentation at the American Meteorological Societys 2015 Annual Meeting.

## RESULTS

An essential element of the RDF algorithm is the import of real observations, derived from ship-board EM-propagation equipment, that are merged with NWP output. The RFC algorithm has been developed so that it can be readily fed into RDF. Utilizing SPANDAR radar clutter maps from the WALLOPS 2000 field campaign, we have processed real observations that are coincident in time and space with in situ measurements of the atmosphere, to understand the efficacy of our algorithms. Figure 1 describes the method of RFC, and how it is incorporated into RDF. The radar clutter for a single sweep of the SPANDAR radar is used as input for RFC. Along the 135 degree radial from Wallops Island, which is coincident with the location of in situ observations, the radar loss as a function of distance (line in figure) is fit to a library of loss patterns and their associated duct properties. The five best-fit loss patterns are displayed with the observations in Fig 1b, and the corresponding profile of modified refractivity that each loss pattern is associated with is displayed in Fig 1a. It is the diagnostic parameters that define these profiles that are then ingested into RDF. We currently are using the best fit profile, but utilization of quality of fit of each profile can help build better estimates of uncertainty in the propagation domain.

An important aspect of RDF is that it can ingest the RFC-derived observation of any subset of the diagnostic properties in one direction, and update the diagnostic properties across the entire area of interest. In order to accomplish this, we explore how the observed value of one diagnostic parameter relates to the other parameters both at the location of the constraint, but over the entire domain. For example, if RFC gives us confidence that the M-deficit is a certain value at one location of the domain, we need to understand how that information translates to knowledge of the top of the trapping layer both at the same location, and elsewhere. We use ensemble NWP simulations to shed light on this problem. For the WALLOPS campaign, a 32-member ensemble of COAMPS simulations was generated from varying initial boundary conditions. This gives an idea of how variability in each diagnostic parameter relates to variability in another parameter at a given location. Figure 2 shows the correlation coefficient between six diagnostic parameters across the 32 ensemble members for a single 12-hour forecast on May 01, 2000. The relationships that we derive here are dependent on the overall meteorological domain, and have different values at other times. We have created a single covariance matrix for use on all observations from the ensemble runs. In addition to understanding the covariance at a single location, it is important to extend this across the entire domain of interest. Figure 3 shows the same covariance calculation, but extends it across our entire NWP domain. In this figure, the colors represent the correlation across the ensemble members between the values at the center of the domain (white square) of the diagnostic variable listed at the top of each column with the values of the diagnostic variable listed next to each row at each point in the domain. This demonstrates that there is spatial inhomogeneity with respect to the covariance, and that these patterns are regime-dependent (not shown). An important area of future research is to determine how much information about these covariance matrices is needed for accurate prediction, and can meteorological information guide the selection a best covariance relationship.

Utilizing the profiles of meteorological variables from the helicopter measurement from WALLOPS

2000, we compare the ability of RDF to replicate the observed profiles of modified refractivity. Figure 4 displays the profiles of modified refractivity as a function of range from Wallops Island due southeast from the helicopter observations (Fig. 4a), the RFC algorithm applied to a SPANDAR radar retrieval (Fig. 4b), and COAMPS 12-hour prediction prior to (Fig. 4c) after (Fig. 4d) implementation of RDF for a single observation on May 01, 2000. There is marked improvement in the representation of the duct properties (from Fig. 4c to Fig. 4d) as observed both by the in situ (Fig. 4a) and radar-derived (Fig. 4b) observations. While not all realizations show such pronounced improvement, RDF is an effective method for incorporating radar-derived observations of meteorology, and applying these observations across an area of interest.

The true metric of RDF lay in its ability to improve the prediction of the radar propagation environment. For the same case noted above, we calculate the loss of a radar signal through the environment specified by the profiles of refractivity using the Advanced Propagation Model (APM Figure 5). The inclusion of radar information into the propagation domain, using RFC (Fig. 5b) and RDF using input from RFC (Fig. 5d), adds significant more detail to the propagation domain as compared to the initial COAMPS profiles (Fig. 5c). Both RFC and RDF better match the propagation that would be observed using the helicopter profiles (Fig. 5a). More work is required to ensure a consistent and robust algorithm for a variety of meteorological conditions, and to calculate the precise amount of improvement that occurs by utilizing RDF. Utilizing the propagation data collected during Wallops-2000, we will compare observed propagation with that derived from the RDF implementation.

Diagnostic Variables
M-Excess
Trapping Layer Top Height
Trapping Layer Base Height
dM/dz
M-Deficit
Evaporation Duct Height

*Table 1: List of diagnostic variables derived from numerical weather model output.*

## IMPACT/APPLICATIONS

A trend in radar and radio is to enable tapping of device status and data such as observed power to other devices. For example, clutter power measurements with the SPS-48 E are now provided to down-stream processing to enable display of hazardous weather. RDF in conjunction with inverse methods in EM propagation enables using such data to refine refractivity estimation. This allows a better characterization of the environment for the purpose of prediction of EM propagation, utilizing the equipment (radars, radios, etc.) that are already aboard a ship. The resulting RDF fields could then be inverted into standard meteorological variables and incorporated as additional observations, in what are typically data denied or data sparse over water environments, into mesoscale model data assimilation schemes.

## **TRANSITIONS**

The refractivity data fusion (RDF) has been selected as a Rapid Transition Project under SPAWAR PMW-120 and ONR-322 funding.

## **RELATED PROJECTS**

None.

## **REFERENCES**

- [1] Karimian, A, C Yardim, T Haack, P Gerstoft, WS. Hodgkiss, T Rogers: Towards assimilation of atmospheric surface layer using weather prediction and radar clutter observations, AMS J Applied Meteorology and Climatology, 2013.
- [2] Daley, R., Atmospheric Data Analysis, Cambridge University Press, 1991.
- [3] Kalnay, E., Atmospheric Modeling, Data Assimilation, and Predictability, Cambridge University Press, 341 pp., 2003.

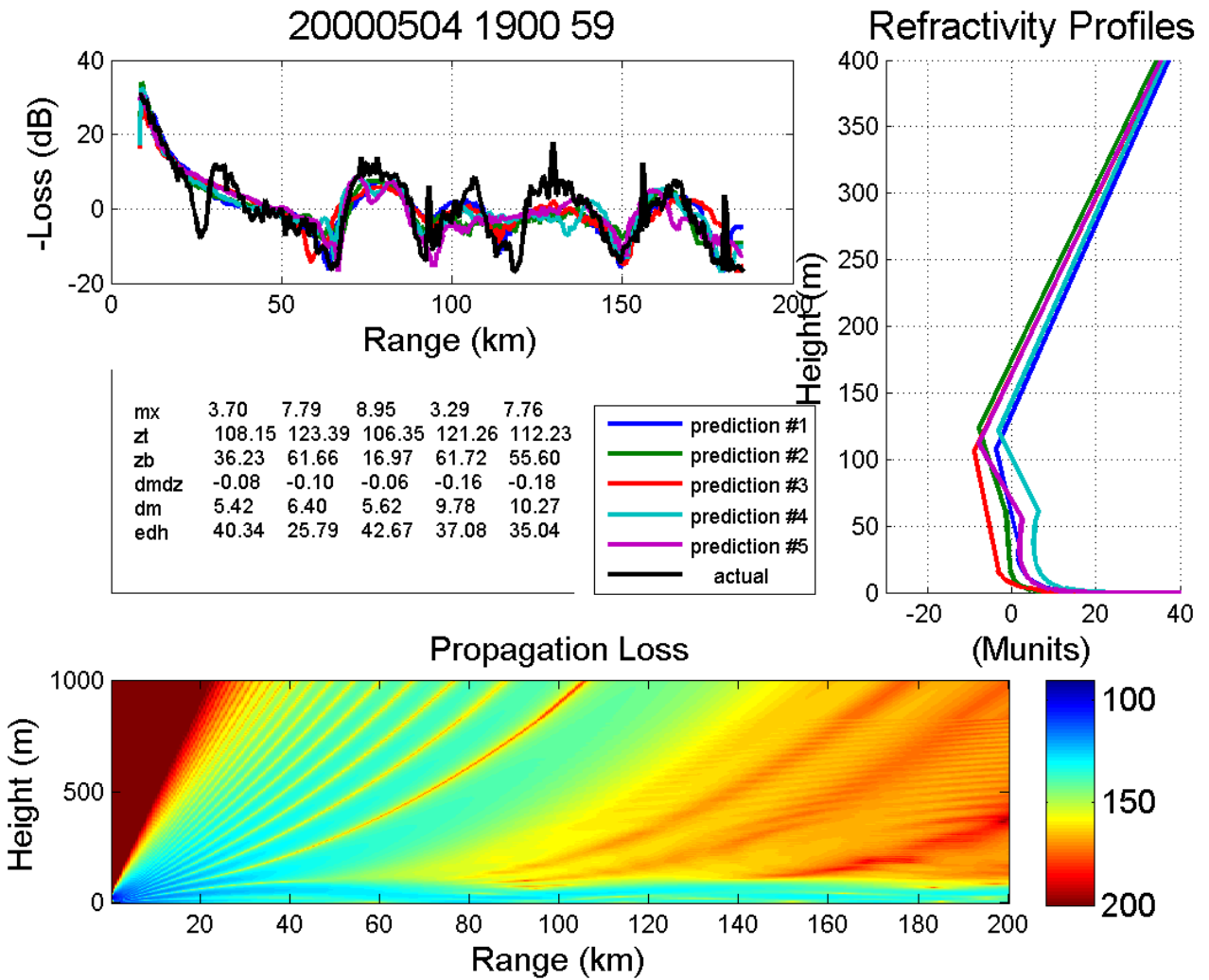


**Figure 1:** (a upper left) The observed radar clutter as a function of range from Wallops Island (black) is compared to the five best fits from the RFC library of propagation loss. (b upper right) The profiles of refractivity associated with the five loss patterns in (a). The diagnostic parameters for the five best fits are shown in the table in the center. (c lower) The propagation loss derived from the APM model for the best RFC prediction (blue line in (a) and (b)).

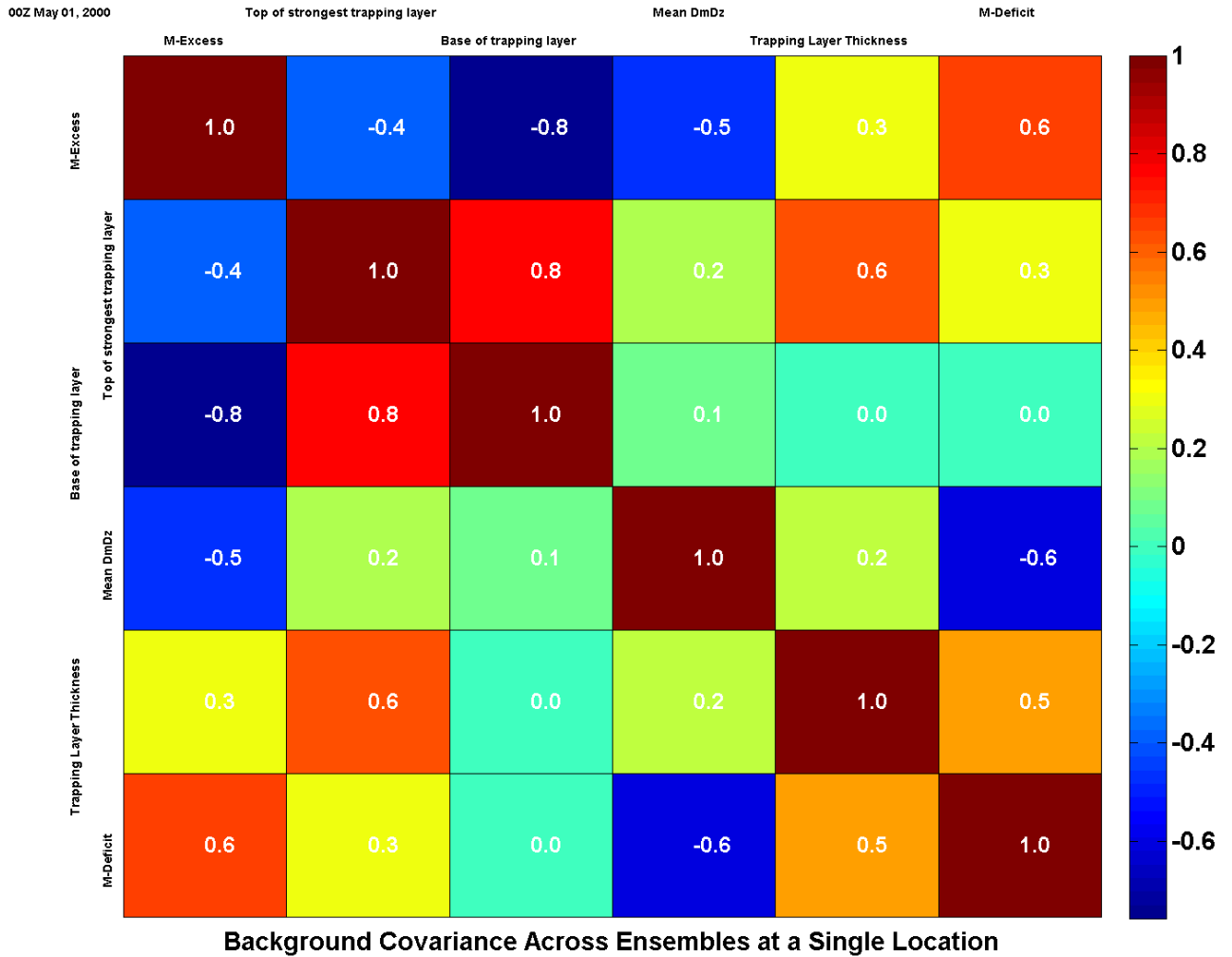


*Figure 2: Correlation coefficient across the 32 ensemble members between the diagnostic parameter on the top, with the parameter on left side for a single point for the 12-hour forecast valid at 12Z on May 01, 2000.*

00Z May 01, 2000

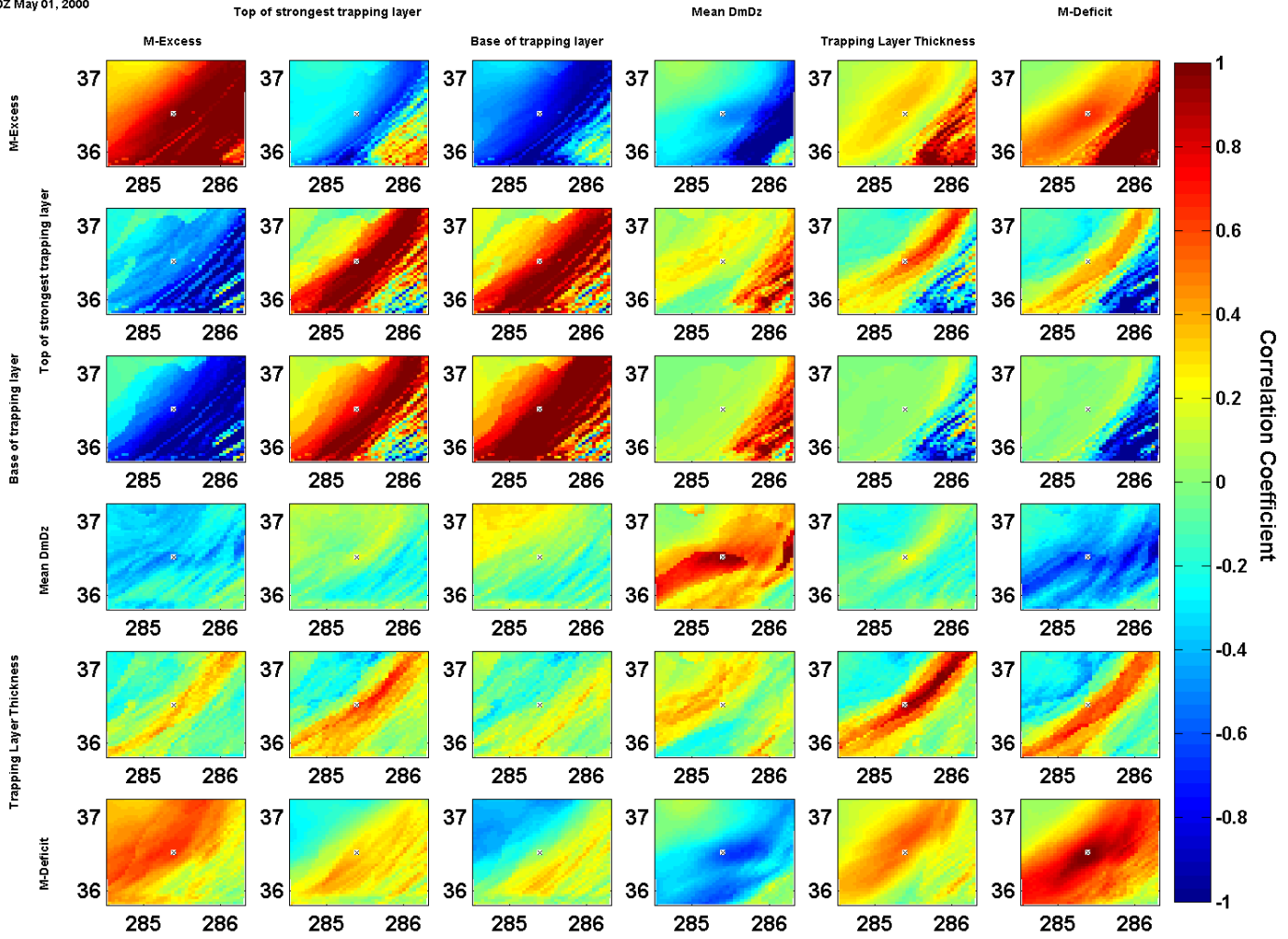


*Figure 3: Correlation coefficient across the COAMPS ensemble members between the value of the diagnostic parameter listed on the top at the center of the domain (black cross) with the value of the diagnostic parameter on the left side at each grid box in the domain.*

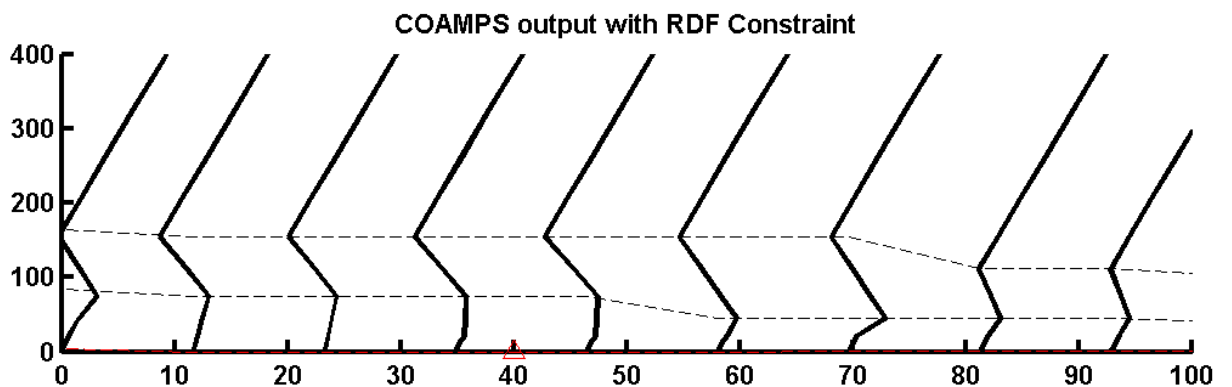
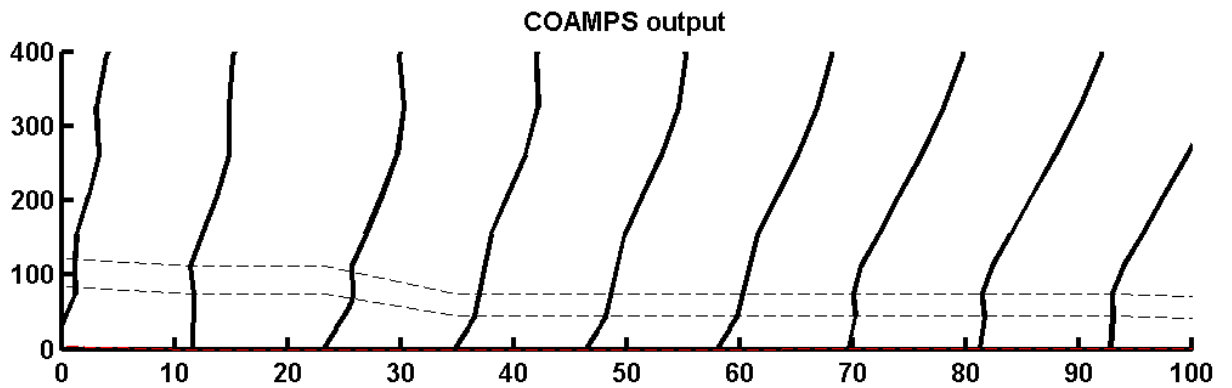
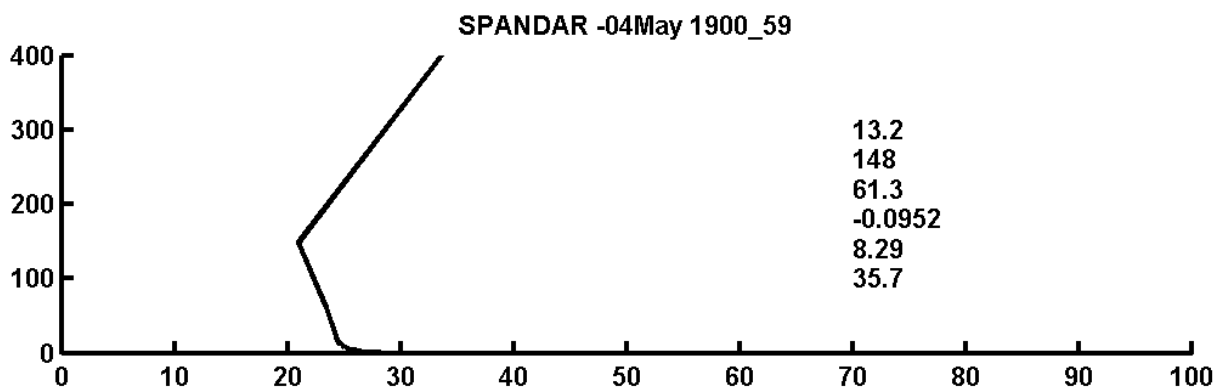
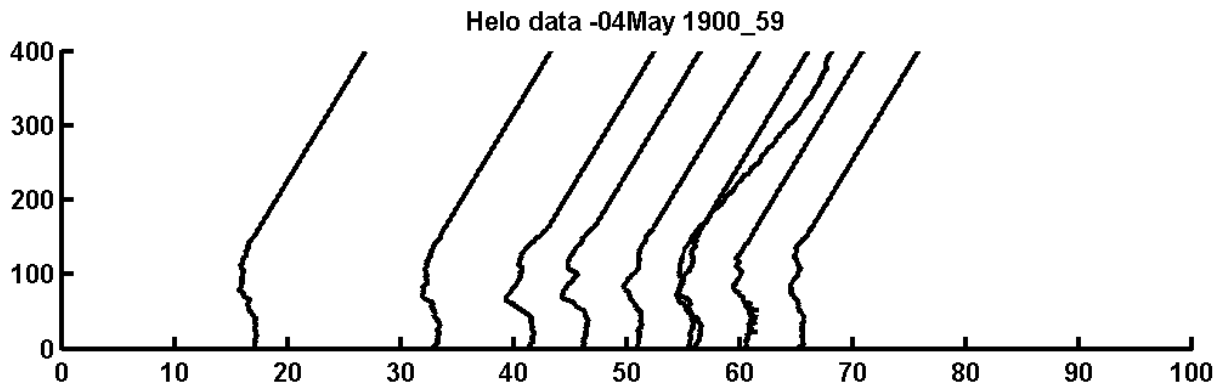
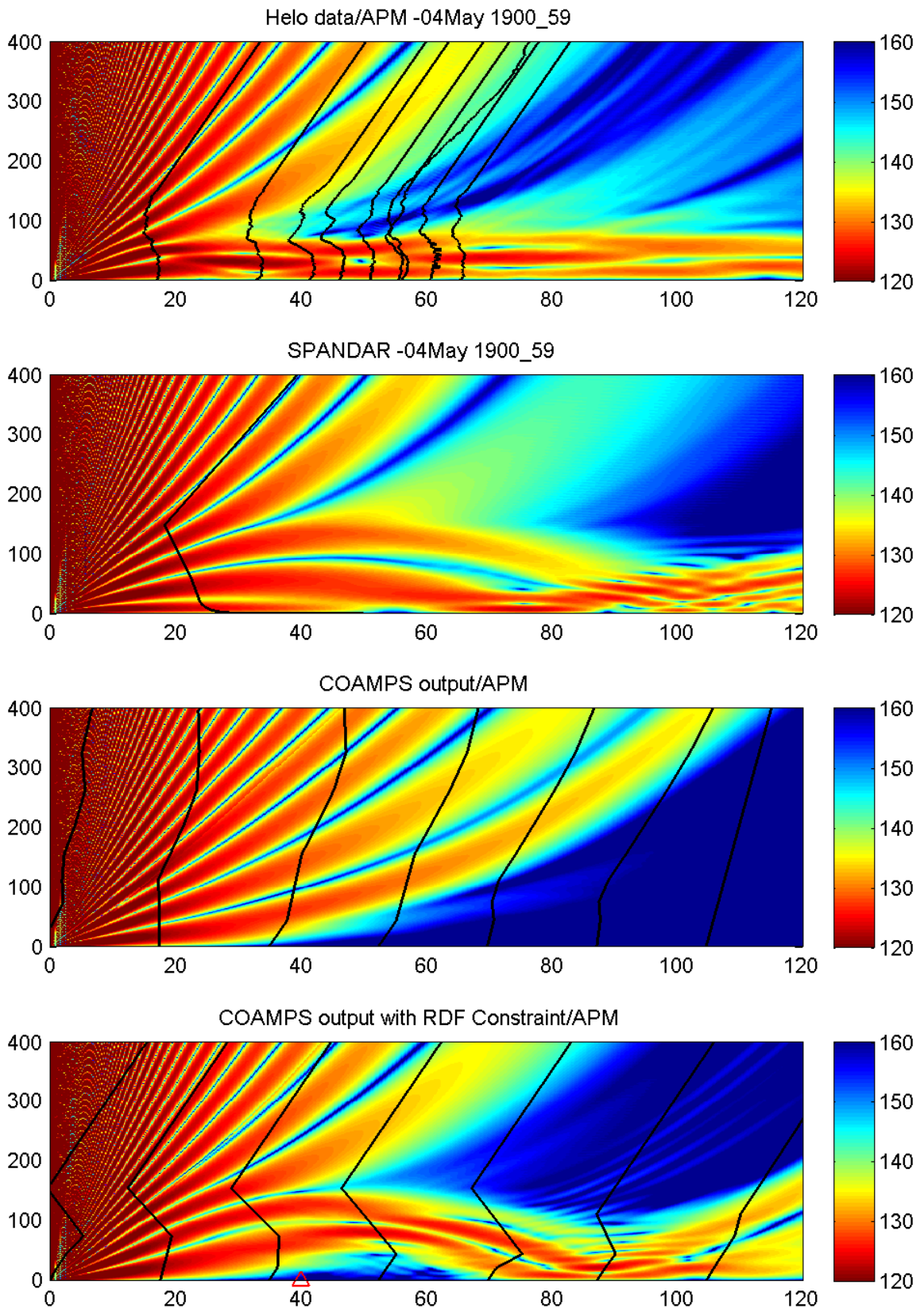


Figure 4: Profiles of modified refractivity as a function of range due southeast from Wallops Island



*Figure 5: Propagation loss (in dB) as a function of range southeast from Wallops Island and height*